

Comprehensive Design and Study on Cogging Torque Reduction in Permanent Magnet Synchronous Motors for Electric Vehicle Technology

Shivani Jitendra Khare¹ and R.S. Ambekar²

¹Department of Electrical Engineering, ²Assistant Professor, Bharati Vidyapeeth (Deemed to be University), College of Engineering, Pune, India.

ABSTRACT

Owing to high efficiency, high power density, high torque to current ratio and high power to weight ratio, application of Permanent Magnet Synchronous drives has been escalating in electric vehicle traction systems. The major concern arises due to increase in cogging torque ripples. The presence of internal harmonic content leading to noise and vibrational disturbances, greatly sways the smooth operation of the motor. To address this challenge is the key to design of Permanent magnet Synchronous motor. Numerous techniques have been enacted upon for truncating the

cogging torque thereby increasing the efficiency for electric vehicle application. This paper presents an exhaustive study on the methods adopted and proposes an optimised model for analysing the effect of skewing in Interior Permanent Magnet Synchronous Motor. Furthermore, the optimal design conclusions based on the proposed shape optimization were confirmed by finite element analysis (FEA) method carried out on RMxprt tool of ANSYS software.

KEYWORDS: Electric Vehicle, Cogging Torque, Permanent Magnet Synchronous Motor, Finite Element Analysis, Efficiency, Skewing, Design Optimization.

Introduction

Amid the growing concerns of environmental protection and energy consumption, development of electric vehicle technology has gained rapid momentum. Having lost its early competitive edge to Internal combustion engine (ICE) vehicles, various advances in micro-electronics and power electronics have contributed significantly to provide capabilities equivalent to ICE vehicles [1]. With the ongoing hikes in fuel rates and their supply limitations, electric vehicles, being environment-friendly, efficient and reliable, have emerged as an alternate medium for the transportation industry. Hence innovations leading to high performance, integrated propulsion systems and coherent auxiliary power units will contribute significantly towards the achieving the goal.

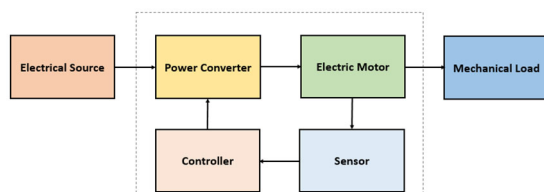


Fig. 1. Block diagram – components of electric vehicle propulsion system

Electric Propulsion is the main aspect of an electric vehicle. The key component affecting the propulsion system are Controller, Converter and Motor [2]. Controller functions to provide proper control signals based on the control methodology to the power electronic devices. Amplified signals operate to switch accurate power electronic devices of the converter which then operates to transfer the power from main supply to the motor leading to propulsion. Motor selection based on the various torque-speed characteristics plays a major role in the process of propulsion. Figure 1 above shows components of electric vehicle propulsion system

Motors for Electric Vehicles

DC motor drives have been employed for propulsion for a prolonged period of time. Due to the hitch of maintenance and shorter life span resulting as an outcome of rubbing of stationary brushes during the process of energy conversion led to decrease in overall efficiency of the motor.

With consecutive developments in microelectronic systems, motor topologies, materials and control algorithms instigated the deployment of AC motor drives over DC counterparts [3]. Pertaining to high efficiency, power density, negligible maintenance and effective regenerative braking phenomenon, AC drives gained

popularity and can be classified as rectangular-fed motors and sinusoidal-fed motors.

Sinusoidal-fed classical Induction motors and Synchronous motors are capable of operating without electronic controllers and can produce persistent instantaneous torque which results to be quite advantageous for certain applications [4]. Field windings of synchronous motors when replaced with permanent magnets form Permanent Magnet Synchronous motors.

Brushless DC motor finds applications in low-power electric vehicle and is expensive. Switched Reluctance motor are known for fault tolerance resulting due to the phenomenon of decoupling of each phase from each other.

This paper constitutes a comprehensive study of Permanent Magnet Synchronous motors and focuses on diverse techniques employed for truncating the cogging torque and torque ripples for enhancing the efficiency of the motor for electric vehicle application.

Permanent Magnet Synchronous Motors

Construction

Permanent magnet synchronous motors (PMSM) are identical to synchronous motor with a variance of rotor as mentioned earlier. High permeability and coercivity materials like Samarium-Cobalt and Neodymium-Iron-Boron are used as permanent magnets which are placed on the rotor core [4]. On the basis of effective position of mounting of permanent magnets, motors are classified into two parts.

- (i) Surface Mounted Permanent Magnet Synchronous Motors (SMPMSM): Magnet is mounted on the surface of the rotor leading to uniform air gap generated as a result of permeability of permanent magnet and air gap being equivalent.
- (ii) Interior Permanent Magnet Synchronous Motor (IPMSM): Magnet is encased inside the rotor thereby increasing robustness. Motor consists of reluctance torque due to presence of saliency.

Figure 2 and 3 below show surface-mounted and interior permanent magnet synchronous motor design, designed on AutoCAD.

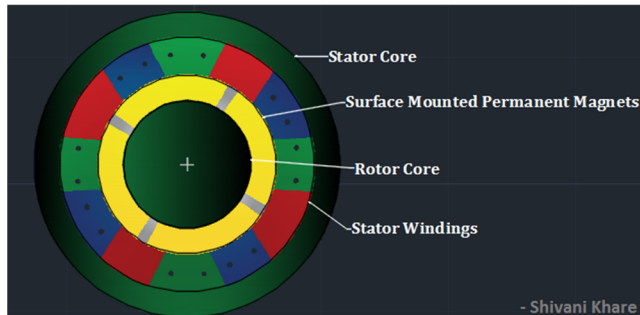


Fig. 2. Surface-Mounted permanent magnet synchronous motor design

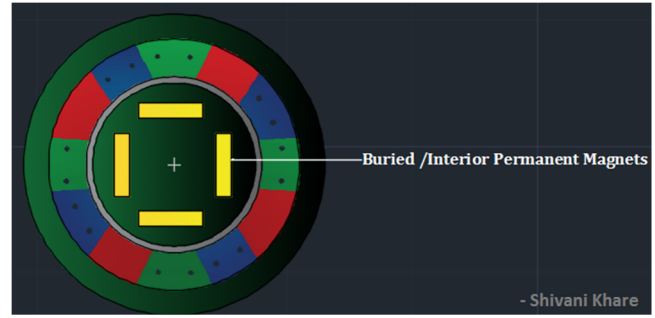


Fig. 3. Interior permanent magnet synchronous motor design on Auto CAD

Working Principle

Depending upon the rotating magnetic field resulting into generation of electromotive force at synchronous speed, stator winding is energized by a three-phase supply. This leads to creation of rotating magnetic field in between the gaps. Upon attaining synchronous speed, rotor field poles lock with the rotating magnetic field in turn producing torque which maintains the rotation of the rotor. PMSM motors are not self-starting and hence it is necessary to impart variable frequency power supply.

Equation for Cogging Torque for permanent magnet synchronous motors

Torque resulting due to interaction between flux of permanent magnet and stator teeth is called as cogging torque. Due to the fact that flux always prefers to flow through low reluctance path, Permanent magnet flux tends to travel through stator teeth resulting in production of unfavourable torque called the cogging torque. This radius-directed, non-uniform torque is responsible for torque ripples, acoustic noise, vibrations in drive systems [5].

Equation for cogging torque can be established by obtaining internal energy of the motor obtained by differentiating magnetic energy with respect to rotor position angle.

$$T_{cogging}(\alpha) = - \frac{\partial W(\alpha)}{\partial \alpha} \quad \text{.....(1)}$$

Where, α is the rotor position angle and W is the magnetic energy.

$$W_\alpha = \frac{1}{2\mu} \int_V B^2 dV \quad \text{.....(2)}$$

Where, B is the magnetic flux density and μ is the permeability.

$$B = G(\theta, z)B(\theta, \alpha) \quad \text{.....(3)}$$

Where, $G(\theta, z)$ is the function of gap permeance and $B(\theta, \alpha)$ is the gap magnetic flux density. θ is the angle along the circumference and α is the angle of rotation.

By substituting Equation 3 in Equation 2 and applying Fourier Series Expansion, the following result is obtained,

$$W_\alpha = \frac{L_s}{4\mu_0} (R_2^2 - R_1^2)$$

$$\left[\sum_{n=0}^{\infty} G_{nN_L} B_{nN_L} \int_0^{2\pi} \cos nN_L \theta \cos nN_L (\theta + \alpha) \right]$$

$$W_{\alpha} = \frac{L_s}{4\mu_0} (R_2^2 - R_1^2) \cdot 2\pi \left[\sum_{n=0}^{\infty} G_{nN_L} B_{nN_L} \cos nN_L \alpha \right] \dots (4)$$

From Equation 1 and Equation 4, we get,

$$T_{cogging}(\alpha) = \frac{L_s \pi}{2\mu_0} (R_2^2 - R_1^2) \left[\sum_{n=0}^{\infty} G_{nN_L} B_{nN_L} nN_L \sin nN_L \alpha \right]$$

Cogging Torque Reduction Techniques

Asymmetric Barrier Design and Inverting Lamination Method

Ki-Chan Kim *et al.* [6] proposes an Asymmetric Barrier Design and Inverting Lamination Method (developed by Taguchi Method) solely for the purpose of minimising the cogging torque and torque ripple generated in Interior Permanent Magnet Synchronous Motor. Detailed analysis has been carried out by implementing Finite Element Analysis to recapitulate and generate accurate computation of torque distortion.

Table 1 below shows the specifications of the motor used for the study. Finite Element Analysis applied on the original model results in cogging torque value to be 3.72 Nm. The author analysed torque ripple on minimum speed of 2750 rpm and maximum speed of 10,000 rpm.

At the minimum speed of 2750 rpm, torque ripple generated at maximum rated torque of 280.43 Nm is computed to be 48.91 Nm which is proportional to torque ripple ratio value of 17.44%. At maximum speed of 10,000 rpm, torque ripple generated at rated torque of 76.96 Nm is computed to be 25.84 Nm which is proportional to torque ripple ratio value of 33.58%. The resulted efficiency of the original model is observed to be 94.96% at the speed of 2750 rpm and 93.21 at the speed of 10,000 rpm. The maximum efficiency detected in the driving range is 97%.

To diminish the cogging torque, author proposes the method of Asymmetric Barrier Design and Inverting Lamination Method (without skewing) and compares the results obtained with the skewed model. The process of lamination is performed on the core of the rotor reversely into two directions without twisting the permanent magnet in axial direction and the barrier is established. Torque analysis is carried out by straight and half axial length model and these waveforms are superimposed to generate final torque waveform. Final torque waveform generated is observed to have torque ripple of 12.7% which is concluded to be less than that of skewed model having torque ripple of 26.07 at maximum speed. The average torque is concluded to have been escalated by 1% as compared with the skew model. Torque ripple reduction by Taguchi method observes reduction to 9.29% and promotion of average torque from 280.43 Nm to 282 Nm.

The author concludes skew method to be good for minimising the torque ripple and the cogging torque but also indicates the problem to average torque reduction and

problem of manufacturing difficulty. As shown in table 2, the proposed method is concluded to increase the average torque and reduce the cogging torque and the torque ripple effectively.

TABLE 1

Motor Specifications

Motor Specifications (Original Model)			
Type	IPMSM	Stator Diameter	115.00 mm
Max Output Power	80 KW	Axial length	135.00 mm
Poles	8	Cogging torque	3.72 Nm
Slots	48	Rotor Diameter	82.50 mm

TABLE 2

Observations for the proposed model

Parameters	Asymmetry	Skew	Origin
Torque (Nm)	282.00	278.00	280.43
Ripple (%)	9.29	10.06	17.44

Method of Increasing the Saliency Ratio and Application of Radial Basis Function and Genetic Algorithm for reduction in cogging torque

Authors in [7] have proposed an optimal design process by considering torque and efficiency in region of constant torque and constant power by application of methodology of maximum torque control in spoke type IPMSM. Constant significant rise in torque and efficiency in the region of constant power is achieved by improving the saliency ratio as compared with the initial model. Maximum Torque per ampere (MPTA) control takes place in region of constant torque and flux weakening (FW) process occurs in region of constant power. For the purpose of computation of cogging torque, Finite Element method (FEM) has been employed followed by Radial Bias Function (RBF) and Genetic Algorithm (GA). Saliency Ratio has been considered as the most important parameter for high power factor and constant power speed range. With the aim of truncating the cogging torque and enhancing the control attributes, the author proposes an optimal design wherein torque and efficiency are analysed by MPTA control in constant torque at 2000 rpm, and FW in constant power region at 4000 rpm by application of d-q equivalent circuits. The motor specifications of the originally used motor is as shown in table 3 below.

i_d related i_q for MPTA and FW control is given as:

$$i_q = \sqrt{I_{sm}^2 - i_d^2}$$

Latin Hypercube Sampling (LHS) wherein input variable range of each variable is split up into intervals and by the process of random sampling, one observation is made on each input variable from intervals. LHS is concluded to be more accurate than random sampling since each input variable has its entire range represented. The design variables of the optimised model when compared with the original model at speed of 2000 rpm depict efficiency and torque to be improved by 3.728% and 4.701% respectively. At 4000 rpm, efficiency and torque show an improvement by 7.151% and 6.937% respectively. The cogging torque when compared with the initial model

shows a reduction of 52.518%. The results are summarised in table 4 below.

TABLE 3

Motor Specifications

Motor Specifications (Original Model)			
Type	IPMSM	Slots	12
Max Output Power	4500 W	Rated Torque	29.5 Nm
Poles	8	Rated Speed	2000 rpm

TABLE 4

Observations for the proposed model

Model	Efficiency (%)	Torque (Nm)	Efficiency (%)	Torque (Nm)	Cogging Torque
Initial	88.623	29.355	81.427	16.939	2.6692
Optimised	91.927	30.735	87.250	18.114	1.2674

Optimal Stator Skewed slot analytical method for cogging torque reduction in surface - interior permanent magnet synchronous motor (SIPMSM)

Authors in [8] have worked to analyse the characteristics of SIPMSM and reduce the cogging torque of the motor. For this purpose, the authors have adopted the design involving stator skewed slots. Cogging torque, back Electromotive force (back-EMF), torque ripple, efficiency and power factor are analysed by 3-dimensional Finite Element Method (3D-FEM) of SIPMSM with stator skewed slots. For the purpose of generating series-parallel equivalent magnetic circuit models (EMCM's) which in turn are employed to design fundamental electromagnetic parameters of SIPMSM, characteristics of the magnetic circuit are taken into account.

The rotor of SIPMSM is such that it contains both SPM and IPM which sum up the magnetic circuit model. SPM and IPM form serial magnetic circuit which is concluded to minimise the magnetic leakage flux thereby amplifying air gap flux density and mechanical strength of the motor. EMCM analysis observes permanent magnets in SIPMSM to have a topological structure whereby serial-parallel EMCM is established which consists of two parallel branches. The maximum cogging torque is observed to be 4.31 Nm. Cogging torque in SIPMSM is given by the equation:

$$T_{cog} = \sum_{m=1,2,3...}^{\infty} Q T_{sc \frac{mN_c}{2p}} \frac{\sin \frac{N_c m N_s \theta_{s1}}{2}}{\frac{N_c m N_s \theta_{s1}}{2}} \sin \left(N_c m a + \frac{1}{2} N_c m N_s \theta_{s1} \right) \quad \dots(5)$$

Cogging torque, in theory is equal to zero when equation 5 is true.

$$N_s = \frac{2k\pi}{N_c m \theta_{s1}} = \frac{k}{m}$$

m Integer

Q Number of stator slot = 24

2p Number of poles = 4

N_c L.C.M. of Q and 2p = 24

k Positive integer

θ_{s1} π/12

On the basis of analytical modelling of cogging torque, it is concluded that SIPMSM contains six-time harmonics. If k=1 and m=1, 6th harmonics of the cogging torque be discarded when skewed slot is set to one slot pitch. Similarly, if m=h and k = 1,2,3...6h, the 6th harmonics is analysed to be eliminated when skewed slot is set for $\frac{1}{6h}, \frac{2}{6h}, \dots, \frac{6h-1}{6h}$ or 1. Hence, authors were successful in concluding elimination of entire cogging torque by skewing of stator slot for slot pitch value of 1.

Authors have compared segment analysis and 3-D FED simulation and analysis methods and have concluded segment analysis to be complicated and inaccurate thereby applying 3-D FED of SIPMSM with stator skewed slots and stator straight slots. The amplitude of cogging torque is contracted by 93.4% in stator skewed slots as compared with the original model. Simulation results in [8] show that cogging torque cannot be entirely eliminated which is in contrast with the result obtained by analytical modelling. Method used for analysis in [8] is affected by interaction between the permanent magnets and the end region of rotor core which can cause a phenomenon in the simulation procedure. Electromagnetic torque of the optimised model observes a reduction of about 0.8%. Torque ripple observes a reduction from 13.02% to 4.54%. Stator skewed slots are concluded to have minimal effect on the maximum torque point. The proposed SIPMSM is observed to have good overload capacity with an over load multiple of about 2.8. Harmonics are observed to be reduced by 47.14% during the experimental verification. Stator skewed slots have no effect on power factor.

Hence it is concluded that stator skewed slots have significant reduction effect on cogging torque and torque ripples and results in improvement of sinusoid and reduction in harmonics of back EMF resulting in significant increase in overload capacity and efficiency.

Authors in [9-10] the authors introduce skewing factor to analyse the skewing effect on cogging torque. The method concluded skewing of stator slots and rotor slots have similar effect on skewing of one torque period, the method fails to deliver practical field distribution for the resultant machine design.

Stator design with Left-shifted and Right-shifted slot opening for truncating the pulsating torque components of Permanent Magnet (PM) Machines

Authors in [11] propose two simple and novel methods for reducing the pulsating torque components of PM machines which involve shifting of slot openings for the reduction of cogging torque and the use of multistage rotor design with flux barriers for reduction in torque ripple. The analysis of torque components is being performed with Finite Element Analysis for the sole purpose of simplifying the efficiency and analysing the effectiveness of applying these methods for Electric Vehicle application. The first method involves a new stator design with unsymmetrical slot opening being applied for optimization of cogging torque for PM machine.

Cogging torque can also be represented in the form of

$$T_{cogging} = \sum_{n=1,2..} T_{c,n} \sin(nN_c \cdot \alpha) \quad \dots(6)$$

It is concluded that larger the N_c , and smaller the number of slots or poles, higher is the cogging torque frequency and smaller is its magnitude [12]. Therefore, it is necessary to have an accurate value of Q and $2p$ (from equation 5). The proposed method is based on compensation method.

Authors in [11] have first considered a stator core with stator slot opening shifted towards right from the centre of the slot with a shift angle of φ_x . Cogging torque is observed to have been shifted towards the right direction, transforming the equation as

$$T_{cogging1} = \sum_{n=1,2..} T_{c,n} \sin [nN_c \cdot (\alpha - \varphi_x)] \quad \dots(7)$$

Likewise, on considering a stator core with stator slot opening shifted towards left from the centre of the slot with a shift angle φ_x , Cogging torque is observed to have been shifted towards left, transforming the equation 6 as

$$T_{cogging2} = \sum_{n=1,2..} T_{c,n} \sin [nN_c \cdot (\alpha + \varphi_x)]. \quad \dots(8)$$

On combining both the techniques to one stator core (either circumferentially or axially), the cogging torques obtained in both the cases compensate each other. For an optimal shifting angle, cogging torque components of the left half and the right half should be shifted by 180° (electrical) and hence the resulting cogging torque can be eliminated completely.

The technique has been applied for stator design of PM magnet for steering application with the specifications shown in table 5 below.

TABLE 5

Motor Specifications

Teeth	12	T_{ripple}	<2% of load Torque
Pole	10	$T_{cogging}$	0.4 Nm (p-p)
T_{max}	18 Nm	n_{max}	1000 rpm

Cogging torque for original design is calculated to be 0.4 Nm (p-p). By applying the new design, it can be concluded that for an optimal shift angle chosen, cogging torque results in a value lower than that of 0.065 Nm (p-p). Authors in [11] successfully conclude the new design to be cheaper and to deliver a high efficiency solution for applications where low cogging torque and low torque ripple are of prime importance.

Authors also propose a novel rotor design for the purpose of torque ripple reduction wherein for a specific phase angle, a shift in torque ripple using unsymmetrical flux barriers has been carried out in the core of the rotor. The basic process applied is similar to that of the previous suggested method. The rotor is axially divided into two parts and mounted on a single rotor shaft. Ripples generated from the rotor parts are shifted for a specific phase angle. For an optimal phase angle, torque ripples can be entirely eliminated.

It can be concluded that by application of the new rotor design, torque ripples of the PM machine are truncated by about of 3.8% of the average torque. This method does not

affect the average torque negatively and hence overcomes the disadvantage of skewing method. With the proposed design, manufacturing of rotor is easier and cheaper as compared with the skewing technique due to the fact that slot shape in the proposed design for PM is similar along the axial length of the machine. Hence, the proposed design the efficient to be adopted.

Proposed Design for Analysing the Effect of Skewing in Permanent Magnet Synchronous Motor

This paper proposes an optimised design model for analysing the effect of change in skewing width on Permanent Magnet Synchronous Motor. The analytical design and its simulation have been carried out using RMxprt tool of Ansys software.

Parameters for optimised design

The final electromagnetic parameters chosen for simulation of the optimised model for analysis are as shown in Table 6 below.

TABLE 6

Motor Specifications considered for analysis

Rated Power (KW)	30
Rated Voltage (V)	320
Number of Poles	10
Length of stator core (mm)	1000
Outer Stator Diameter (mm)	275
Inner Stator Diameter (mm)	178
Stator Slot fill factor (%)	62.6174
Stator Winding factor	0.955
Number of stator slots	48
Length of rotor (mm)	1000
Number of phases	3
Number of turns	24
Number of parallel branches	1
Synchronous speed (rpm)	3000
Number of conductors per slot	3
Average coil pitch	4

Model Design

The optimised model designed by considering the above parameters is shown in figure 4.

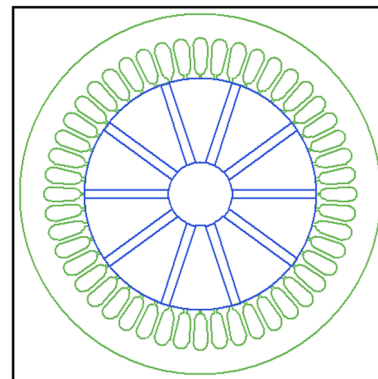


Fig. 4. Optimised design for PMSM analysis

Simulation Results

Case 1: Skew Width (Number of slots) is 1

Skew Width when considered as 1 produces a cogging torque of 3.55553×10^{-12} N-m. The no load input power of 466.485 W. Efficiency of the motor is observed to be 98.1463% and Maximum output power of 38669.8 W is obtained. Total loss of 566.669 W is observed. Figure 5 below shows cogging torque in 2 teeth. Figure 6 below shows variation of power with the torque angle. Figure 7 below shows variation of Efficiency with the torque angle. Figure 8 below shows Phase voltage under loaded condition.

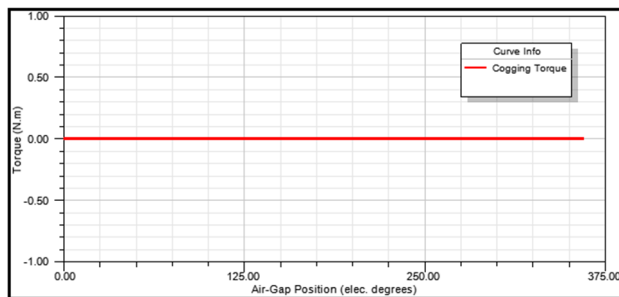


Fig. 5. Cogging torque in 2 teeth

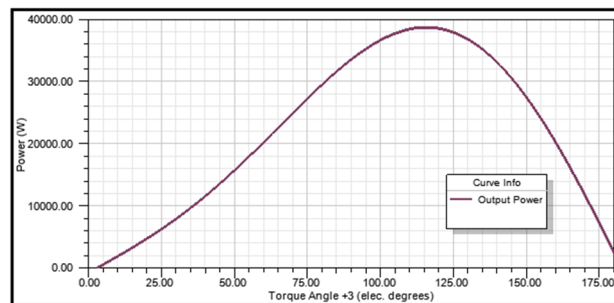


Fig. 6. Variation of out-put power with torque angle

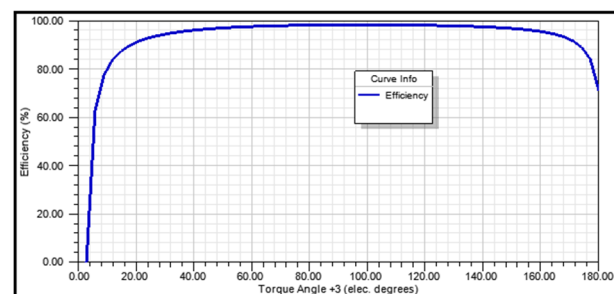


Fig. 7. Variation of efficiency with torque angle

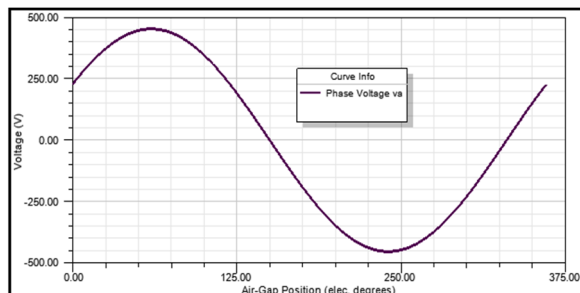


Fig. 8. Variation of phase voltage under loaded condition

Case 2: Skew Width (Number of slots) is 2

Skew Width when considered as 2 produces a cogging torque of 3.55553×10^{-12} N-m. The no load input power of 467.659 W. Efficiency of the motor is observed to be 98.1278% and Maximum output power of 37021.2 W is obtained. Total loss of 572.519 W is observed. Figure 9 below shows cogging torque in 2 teeth. Figure 10 below shows variation of power with the torque angle. Figure 11 below shows variation of Efficiency with the torque angle. Figure 12 below shows Phase voltage under loaded condition.

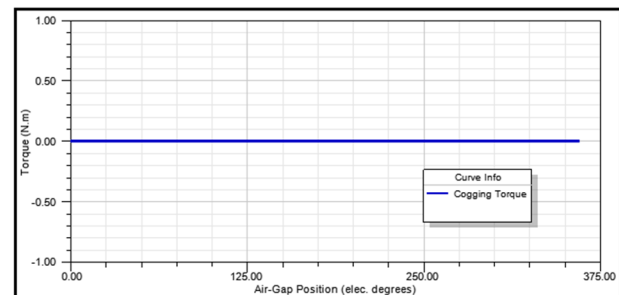


Fig. 9. Cogging torque in 2 teeth

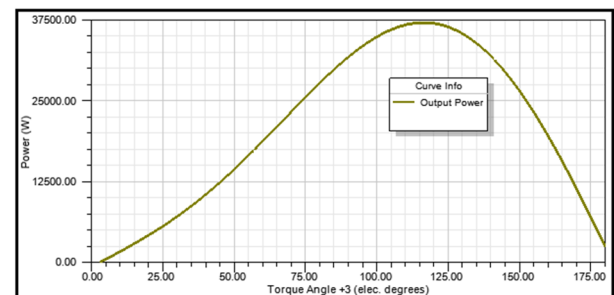


Fig. 10. Variation of output power with torque angle

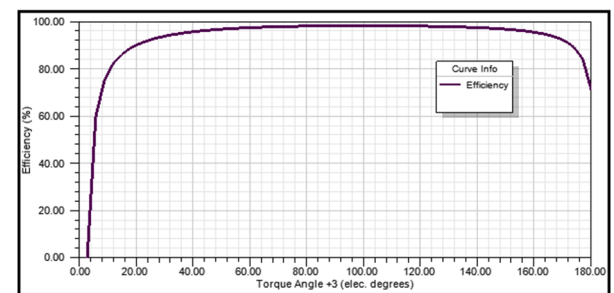


Fig. 11. Variation of efficiency with torque angle

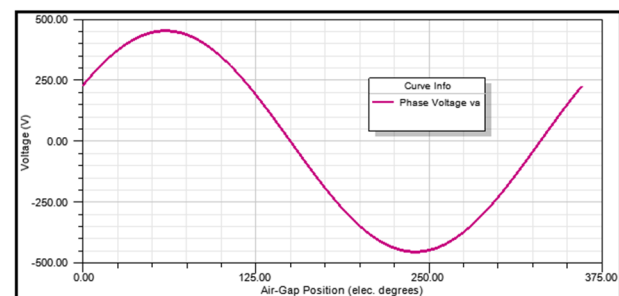


Fig. 12. Variation of phase voltage under loaded condition

TABLE 7
Simulation results

Parameter	Model with Skew Width = 1	Model with Skew Width = 2
No-Load Line Current (A)	15.6264	18.9157
No-Load Input Power (W)	466.485	467.659
Maximum Line Induced Voltage (V)	369.546	341.845
Specific Electric Loading (A/mm)	9.48067	9.73068
Armature Current Density (A/mm ²)	0.881407	0.90465
Armature Copper Loss (W)	109.473	115.323
Total Loss (W)	566.669	572.519
Output Power (W)	30002.1	30007.8
Efficiency (%)	98.1463	98.1278
Rated Torque (N-m)	95.4998	95.5178
Maximum Output Power (W)	38669.8	37021.2

Observations

Table 7 above displays the simulation results obtained by simulating the Interior mounted permanent magnet synchronous motor with an increased skewing width. On comparing the results obtained by simulating the IPMSM model with skewing width of 1 and skewing width of 2, following observations can be made:

- On incrementing the skewing width by a factor of 1, maximum output power obtained decreases by 4.35% as compared to the initial model.
- Rated torque obtained is 95.5 N-m.
- Armature Current density is observed to increase by 2.602% of the initial model.
- Total loss increases by 1.02% on increasing the skewing factor by 1.
- Maximum induced voltage is observed to reduce by 7.78% as compared with initial model.
- Efficiency observes a very small change when skew width of the motor is increased.

Conclusion

This paper presents a comprehensive study on various methods employed for the primary purpose of reducing the cogging torque of Permanent Magnet synchronous machine. Furthermore, an optimised model has been proposed for the sole purpose of analysing the effect of variations in skew width on various parameters. Results obtained from finite element analysis using RMXprt tool of ANSYS software confirms efficiency of 98.1%, rated torque of 95.5 N-m and a change of 4.35% in output power of the machine. It can be concluded that skew method is useful in reducing the torque as concluded by the comprehensive study, but increasing the skew of the

motor does not have any significant change in the value of cogging torque.

References

- [1] C. C. Chan, "An overview of electric vehicle technology," in *Proceedings of the IEEE*, vol. 81, no. 9, pp. 1202-1213, Sept. 1993, doi: [10.1109/5.237530](https://doi.org/10.1109/5.237530).
- [2] K. W. E. Cheng, "Recent development on electric vehicles," 2009 3rd International Conference on Power Electronics Systems and Applications (PESA), 2009, pp. 1-5.
- [3] M. S. Patil and S. S. Dhamal, "A Detailed Motor Selection for Electric Vehicle Traction System," 2019 Third International conference on I-SMAC (IoT in Social, Mobile, Analytics and Cloud) (I-SMAC), 2019, pp. 679-684, doi: [10.1109/I-SMAC47947.2019.9032616](https://doi.org/10.1109/I-SMAC47947.2019.9032616).
- [4] A. Loganayaki and R. B. Kumar, "Permanent Magnet Synchronous Motor for Electric Vehicle Applications," 2019 5th International Conference on Advanced Computing & Communication Systems (ICACCS), 2019, pp. 1064-1069, doi: [10.1109/ICACCS.2019.8728442](https://doi.org/10.1109/ICACCS.2019.8728442).
- [5] C. Studer, A. Keyhani, T. Sebastian and S. K. Murthy, "Study of cogging torque in permanent magnet machines," IAS '97. Conference Record of the 1997 IEEE Industry Applications Conference Thirty-Second IAS Annual Meeting, 1997, pp. 42-49 vol.1, doi: [10.1109/IAS.1997.643006](https://doi.org/10.1109/IAS.1997.643006).
- [6] K. Kim, "A Novel Method for Minimization of Cogging Torque and Torque Ripple for Interior Permanent Magnet Synchronous Motor," in *IEEE Transactions on Magnetics*, vol. 50, no. 2, pp. 793-796, Feb. 2014, Art no. 7019604, doi: [10.1109/TMAG.2013.2285234](https://doi.org/10.1109/TMAG.2013.2285234).
- [7] Y. Son, K. Hwang and B. Kwon, "Maximum torque control for optimal design to reduce cogging torque in spoke type interior permanent magnet synchronous motor," 2010 IEEE Energy Conversion Congress and Exposition, 2010, pp. 3654-3658, doi: [10.1109/ECCE.2010.5618309](https://doi.org/10.1109/ECCE.2010.5618309).
- [8] J. Si, S. Zhao, L. Zhang, R. Cao and W. Cao, "The characteristics analysis and cogging torque optimization of a surface-interior permanent magnet synchronous motor," in *Chinese Journal of Electrical Engineering*, vol. 4, no. 4, pp. 41-47, Dec 2018, doi: [10.23919/CJEE.2018.8606788](https://doi.org/10.23919/CJEE.2018.8606788).
- [9] N. Bianchi and S. Bolognani, "Design techniques for reducing the cogging torque in surface-mounted PM motors," in *IEEE Transactions on Industry Applications*, vol. 38, no. 5, pp. 1259-1265, Sept.-Oct. 2002, doi: [10.1109/TIA.2002.802989](https://doi.org/10.1109/TIA.2002.802989).
- [10] L. Zhu, S. Z. Jiang, Z. Q. Zhu and C. C. Chan, "Analytical Methods for Minimizing Cogging Torque in Permanent-Magnet Machines," in *IEEE Transactions on Magnetics*, vol. 45, no. 4, pp. 2023-2031, April 2009, doi: [10.1109/TMAG.2008.2011363](https://doi.org/10.1109/TMAG.2008.2011363).
- [11] G. Dajaku and D. Gerling, "New methods for reducing the cogging torque and torque ripples of PMSM," 2014 4th International Electric Drives Production Conference (EDPC), 2014, pp. 1-7, doi: [10.1109/EDPC.2014.6984396](https://doi.org/10.1109/EDPC.2014.6984396).
- [12] Z. Q. Zhu and D. Howe, "Influence of design parameters on cogging torque in permanent magnet machines," in *IEEE Transactions on Energy Conversion*, vol. 15, no. 4, pp. 407-412, Dec. 2000, doi: [10.1109/60.900501](https://doi.org/10.1109/60.900501).

Address correspondence to: Mr. Shivani Jitendra Khare, Department of Electrical Engineering, Bharati Vidyapeeth (Deemed to be University), College of Engineering, Pune, India.
Email: shivani.khare-coep@bvucpep.edu.in